Numerical modeling of sand migration during gas production from gas hydrate reservoir in the Prudhoe Bay Unit on the Alaska North Slope

Shun Uchida[1,2,*], Yongkoo Seol[2], Koji Yamamoto[3]

[1]*Rensselaer Polytechnic Institute, USA*
[2]*National Energy Technology Laboratory – U.S. Department of Energy, USA*
[3]*Japan Oil, Gas and Metals National Corporation, Japan*
*Corresponding Author: uchids@rpi.edu

ABSTRACT

Recent field-scale tests have demonstrated, despite a short period of time, feasibility of gas production from gas hydrate reservoir. As a next step, Japan-US collaborative team plan to conduct 12-18 months of continuous gas production from a high-quality gas hydrate reservoir, located in the Prudhoe Bay Unit, Alaska North Slope. However, as has been observed in the past field-scale tests, excessive sand migration into the well could hinder the potential long-term gas production. Furthermore, despite advancement of numerical modeling, inherent uncertainties in the site conditions and in-situ properties make an accurate prediction challenging. Therefore, it is important to better understand how sand migration could occur such as where its main source of sand is and what properties control the sand flow. Utilizing a thermo-hydro-mechanical sand migration model, this paper studies the behavior of the hydrate reservoir in the Prudhoe Bay Unit during one-year long gas production via depressurization. The results show that sands mainly come from sand and clay interfaces near the well and also that the dominant properties appear to change over time due to continuously changing reservoir responses. This finding suggests that the effect of sand migration may not be negligible and thus further studies are necessary.

Keywords: gas hydrates, sand migration, energy recovery, Alaska North Slope, numerical modeling

NONMENCLATURE

Symbols	
ϵ_d	deviatoric strain
κ	slope of reloading line
λ	slope of isotropic compression line
ν	Poisson's ratio
ω_3	hydrate factor for critical gradient
ω_4	deformation to mobilization potential
σ'_h	horizontal effective stress
σ'_z	vertical effective stress
E_h	increase in stiffness due to hydrate
i_{crtw}	critical hydraulic gradient (no hydrate)
i_w	hydraulic gradient of water
$\mathbf{K}$	intrinsic permeability tensor
K_0	in-situ earth coefficient (= $\sigma'_{h0}/\sigma'_{z0}$)
$\mathbf{K}_h$	effective permeability = $\mathbf{K}(1-S_h)^N$
M	critical state stress ratio (= q_{crt}/p'_{crt})
M_p	sand mobilization potential
n	porosity
p'	mean effective stress
p'_{cd}	hydrate dependent soil strength
p'_{cs}	preconsolidation stress
P_w	pore water pressure
q	deviator stress
$\mathbf{q}_w$	water flux vector
S_h	hydrate saturation
S_h^{mec}	mechanical hydrate saturation
T	temperature
t	time
u	pre-yield plasticity factor
V_{fs}	volume of flowing sands
V_s	sand volume (= V_{ss} + V_{fs})
V_{ss}	volume of stationary sands
V_w	volume of water

1. INTRODUCTION

Gas hydrates in deep sediments, especially sandy sediments, have been identified one of the highly promising candidates to supply centuries worth global energy because of the compatibility with conventional

gas production technology (e.g. Boswell and Collett, 2011). In addition, their relatively high permeability is suitable to accommodate fluid flow and heat supply, two of essential factors for continuous gas production and hydrate dissociation (e.g. Moridis et al., 2009; Myshakin et al., 2019). As of today, there have been only a limited number of field-scale gas production tests and no test has achieved in continuous and constant-rate gas production longer than a month (e.g. Dallimore et al., 2012; Konno et al., 2017; Chen et al., 2018). One of the major challenges is to control sand flow and, when excessive, it could lead to shutting in a production well as observed in some of these tests (e.g. Yamamoto et al., 2019). Motivated by the incidents, Uchida et al. (2016a) developed a thermo-hydro-mechanical sand migration model to simulate sand migration phenomenon in gas hydrate reservoir and it was applied to understand how sand migration could occur in various hydrate reservoir settings during gas production for a period of as long as one month (e.g. Uchida et al., 2019a). One of the key findings is that sand migration does not appear to stabilize due to ongoing non-uniform hydrate dissociation because it keeps sediments' strains and hydraulic gradient evolving throughout gas production. As Japan-US collaborative team plans to conduct one-year long gas production test in the Prudhoe Bay Unit, analyses for a longer period are required to better understand the effect of sand migration on the reservoir behavior.

This paper presents thermo-hydro-chemo-mechanical simulations of one-year long gas production from hydrate reservoir in the Prudhoe Bay Unit, focusing particularly on where sands come from. The analyses also determine the effect of variability in in-situ conditions such as permeability and mechanical properties on sand migration. This is because these properties tend to possess inherent uncertainties. It is also because these data are not readily available as only a few state-of-the-art pressure coring tool such as hybrid pressure-coring system by Kubo et al. (2014) and associated core analyzing devices such as PCCTs (e.g. Santamarina et al., 2015), PICATS (e.g. Priest et al., 2019), and TACTT (e.g. Yoneda et al., 2017, 2019) are deemed capable of providing high-quality hydrate-bearing sand samples. The results could therefore help to prioritize which property should be evaluated with limited samples. The next section describes modeling procedure including a brief overview of the adopted sand migration model that is modified after Uchida et al. (2016a), model geometry and initial thermo-hydro-chemo-mechanical conditions. A section of results and discussions follows and then concluding remarks are provided.

2. MODELING PROCEDURE

2.1 Overview of modified sand migration model

Sand migration phenomenon in gas hydrate reservoir undergoes complex multiphysics processes. As a result, the model developed by Uchida et al. (2016a) required six parameters that would be difficult to be determined. Although these six parameters are necessary from analytical view points, to have better engineering perspective, Uchida et al. (2019b) investigated the effect of each parameter on sand production (i.e., sand flow collected at the well) in an idealized hydrate reservoir. Three parameters have been found dominantly determining the extent of sand production and, accordingly, the thermo-hydro-mechanical sand migration model can be modified as follows.

Reduced from three, there are now two states of sands:

$$V_s = V_{ss} + V_{fs} \tag{1}$$

where V_s is the volume of sands, V_{ss} is the volume of stationary sands and V_{fs} is the volume of flowing sands. The stationary sands will change their state into flowing sands when mobilized. The model assumes that mobilization initiates when subjected to larger hydraulic gradient than the critical value and its volume is proportional to the remaining volume of stationary sands, V_{ss}, and mobilization potential, M_p. These can be mathematically expressed as:

$$dV_{ss} = -V_{ss} M_p H\left(\frac{i_w}{i_{crt}} - 1\right) dt \tag{2}$$

where $H(\cdot)$ is the heaviside function that provides initiation of sand mobilization when $i_w/i_{crt} > 1$, i_w is the magnitude of hydraulic gradient vector of water (= $|\mathbf{i}_w|$), i_{crt} is the critical hydraulic gradient for sand mobilization to occur, t is time and M_p is the mobilization potential. The mobilization potential is assumed to increase with shear deformation of the sediments so that:

$$M_p = \omega_4 \epsilon_d + \ln\left(\frac{V_{ss}}{V_{s0}}\right) \tag{3}$$

where ω_4 is the parameter to convert strain to mobilization potential, ϵ_d is the deviatoric strain, V_{s0} is the initial sand volume. Eq. (3) states that, while the potential increases with sediment shear deformation, actual mobilization (i.e., $\ln(V_{ss}/V_{s0})$ being negative) depletes the mobilization potential, eventually leading to cease of sand mobilization. With presence of hydrate, hydrate-bearing sands could resist being mobilized. The model assumes, therefore, that the critical hydraulic gradient increases with hydrate saturation such that:

$$i_{crt} = \frac{i_{crtw}}{(1-S_h)^{\omega_3}} \tag{4}$$

where i_{crtw} is the critical hydraulic gradient for sand mobilization in fully water-saturated condition, S_h is the hydrate saturation and ω_3 is the parameter to increase i_{crt}

according to Sh. Sand mobilization directly increases the volume of flowing sands. Flowing sands travel with water by the form of sand-water mixture (suspension) and the amount of incoming and outgoing flowing sands alter the volume of flowing sands in a given location. These two factors contribute to the change in the volume of flowing sands:

$$dV_{fs} = -dV_{ss} - \boldsymbol{\nabla} \cdot \left(\frac{V_{fs}}{V_w}\mathbf{q}_w\right) V dt \quad (5)$$

where V_w is the volume of water, V is the control volume and $\mathbf{q}_w$ is the volumetric water flux vector given by the Darcy's law by assuming that the sand-water mixture holds the same volumetric flux with water and flowing sands. The incremental form of Eq. (1), that is, the change in the sand volume dV_s, can be given by summing Eq. (2) and Eq. (5) together and is solely caused by the sand flow.

The modified sand migration model is now defined by three parameters, ω_3, ω_4 and i_{crtw}. It suggests that sand migration increases with hydraulic gradient and deformation but decreases with presence of hydrate. The change in the sand volume dV_s by migration is coupled with other thermo-hydro-chemo-mechanical components. For example, heat travels with sand flow, the change in the sand volume alters pore pressure, which affects hydrate dissociation rate and the effective stress, and also it causes plastic volumetric deformation. The detailed descriptions of how dV_s is coupled are provided in Uchida et al. (2016a).

2.2 Model geometry and initial conditions

Fig. 1 presents the considered axisymmetric model geometry for the analysis of sand migration during gas production in the Prudhoe Bay Unit. The hydrate reservoir is assumed to consist of clean sand and located between 848 and 861 m below sea level (bsl), interposed with silty-clay layers. The initial hydrate is assumed to be homogeneously distributed with S_{h0} = 70%. The initial porosity of the hydrate-bearing sediments is n_0 = 0.4, where that of the silty clay is n_0 = 0.3. At the top of the model boundary, which is at the depth of 800 m below sea level, a constant total vertical stress of σ'_z = = 7.6 MPa, a constant pore water pressure of P_w = 8.3 MPa and a constant temperature of T = 281 K are applied. These values incorporate the presence of permafrost from ground level (≈ 20 m above sea level) to the depth of approximately 570 m below sea level. At the initial condition, the total vertical stress, pore pressure and temperature all increase linearly with depth by the gradient of approximately 9.6 kPa/m, 10 kPa/m and 0.04 K/m, respectively. At the bottom of the boundary, the constant pore water pressure (≈ 9.4 MPa) and temperature (≈ 285 K) are applied and no vertical displacement is allowed. At the far-field boundary, which is modeled at r_∞ = 150 m, the constant total stress, pore water pressure and temperature are applied. The horizontal effective stress is assumed to be half of the vertical effective stress, corresponding to the in-situ earth coefficient of K_0 = 0.5 condition. This results in the initial mean effective stress of $p'_0 \approx 5.5$ MPa around the production zone. The well boundary is assumed to be insulated and is mechanically fixed (zero radial displacement). The production zone is assumed to cover the entire hydrate-bearing layer, where flow boundary is open for all water, gas and sand-water mixture.

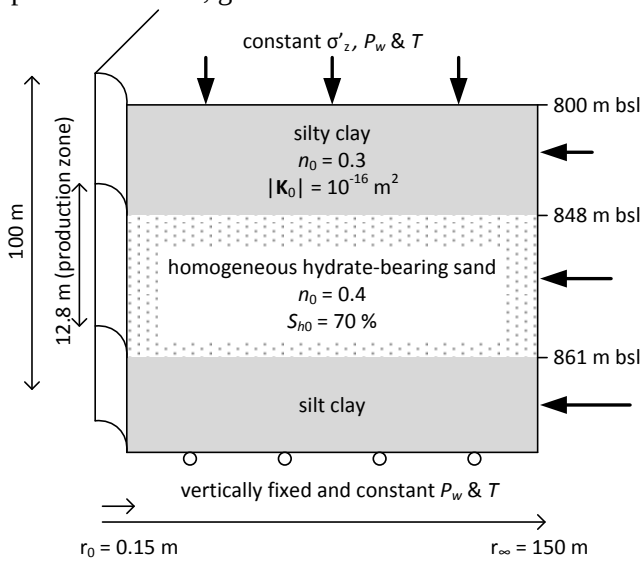

Figure 1. Model geometry and initial conditions.

As described in Eqs. (1)–(5), sand migration is mainly caused by hydraulic gradient and sediment deformation. Therefore, this study facilitates inherent uncertainty existing within the sediments' permeability and stress-strain curve. Fig. 2 presents the considered variability with 95 % of confidence interval in (a) permeability and (b) stress-strain curve. These ranges are based on adopted mean values for corresponding properties summarized in Table 1 and their variance based on 25 % of coefficient of variation.

In specific, for the permeability, the range is determined based on variance in the initial intrinsic permeability, $\|\mathbf{K}_0\|$, and the initial effective permeability (i.e., permeability with hydrate), $\|\mathbf{K}_{h0}\|$. The evolution of the permeability is modeled through a simple power law by Masuda et al. (1999):

$$\mathbf{K}_h = \mathbf{K}(1 - S_h)^N \quad (6)$$

where N is obtained for the initial value and remains constant throughout the analyses. For simplicity, this study assumes that the vertical permeability is the same value as the horizontal permeability.

To construct variation in the stress-strain curves, this study employs the methane hydrate critical state model by Uchida et al. (2012, 2016b). The mean values

presented in Table 1 are obtained by best curve-fitting to the experimental data of high-quality Nankai hydrate-bearing sands by Yoneda et al. (2017), except the initial preconsolidation stress p'_{cs0}. The best fit is achieved by p'_{cs0} = 5.2 MPa for the test data (Uchida et al., 2019a) but the value is lower than an expected value of the in-situ preconsolidation stress around the production zone in the Prudhoe Bay Unit. The expected value can be evaluated under the initial K_0 condition and the critical state stress ratio M assuming that the host soil is normally consolidated and is approximately p'_{cs0} = 7.0 MPa. Based on the parameters with variation, the curves in Fig. 2b are created by simulating triaxial shear for S_{h0} = 70% case and Sh_0 = 0 case. The initial confining stress is set at p'_0 = 5.5 MPa, which is similar value to the initial mean effective stress around the production well.

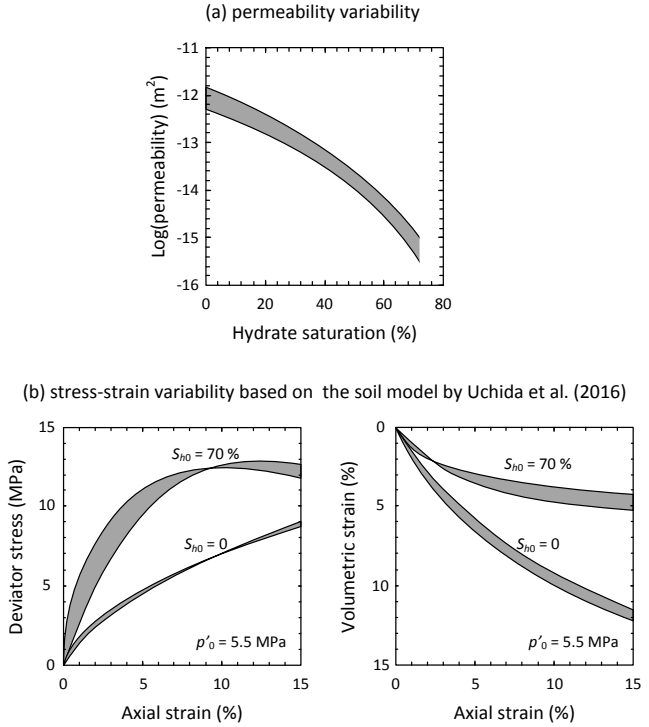

Figure 2. Considered variability in (a) permeability and (b) stress-strain curve under triaxial shear.

3. SAND MIGRATION ANALYSIS OVER A YEAR-LONG GAS PRODUCTION

For gas production and sand migration analyses, pressure drawdown of 6 MPa is applied, that is, a constant well pressure of approximately 2.9 MPa. Fig. 3 presents spatial and temporal changes in (a) pore water pressure, (b) hydrate saturation, (c) stress ratio (q/p') with displacement arrows and (d) the sand volume over a period of one year. Well depressurization causes the pore pressure to drop (Fig. 3a), leading to hydrate dissociation (Fig. 3b). As continuous hydrate dissociation under the constant well pressure requires heat supply due to endothermic nature of hydrate dissociation, hydrate tends to dissociate more in the vicinity of silty-clay layers. This is because silty-clay layer is relatively warmer as there is no hydrate dissociation and thus heat can be transferred via convection and conduction.

Table 1. Varied properties of hydrate-bearing sediments and their mean values adopted in this study.

permeability		
initial intrinsic perm.	$\|\|\mathbf{K}_0\|\|$	10^{-12} m^2
initial effective perm.	$\|\|\mathbf{K}_{h0}\|\|$	10^{-15} m^2
stress-strain		
critical state stress ratio	M	1.42
slope of isotropic comp.	λ	0.26
slope of reloading line	κ	0.013
Poisson's ratio	ν	0.20
ini. preconsolidation stress	p'_{cs0}	7.0 MPa
pre-yield plastic factor	u	2
hydrate dependent strength	p'_{cd}	$97.8(S_h^{mec})^{1.3}$ MPa
mechanical hydrate sat.	S_h^{mec}	$\exp(-6\varepsilon_d^p)S_h$
hydrate dependent stiffness	E_h	$630S_h^{mec}$ MPa

Fig. 3c shows the stress ratio q/p' and the displacement vectors. The stress ratio is indicative of deformation mode such that an increase in the value suggests that the deformation is in shear-orientated while a decrease implies that the deformation is in volumetric. Since the in-situ earth coefficient is K_0 = 0.5, the initial value is q_0/p'_0 = 0.75. Therefore, it can be seen that the sediments near the production zone initially deforms in volumetric manner but with time it deforms in shear and, in particular, the sediments near the interface between sand and silty-clay layer shows a large shear deformation. This is caused by two mechanisms. Firstly, the difference in the sediments' permeability and stress-strain curves between the hydrate-bearing sand and silty-clay layers make the two layers diverge, leading to shearing deformation. This becomes less significant when the two layers' permeability and stress-strain curves are remodeled to be similar. Secondly, preferential hydrate dissociation in the region imposes the sediments under complex stress change. While the sediments loses its effective stress due to hydrate dissociation, leading to the reduction in p', the sediments tend to increase q due to radial deformation (cavity contraction). Therefore, the ratio q/p' increases, resulting in large shearing deformation. Above the production zone, the deformation is mostly volumetric as the value of q/p' decreases. Because of this, the silty-clay layer considerably subsides, almost without any radial displacement. Fig. 3d shows the reduction in the sand volume (negative denotes reduction) over time,

suggesting where sand mobilization mostly occurs. The area with a large reduction corresponds to the area where a significant shear deformation is observed. This highlights the importance of understanding in deformation mechanisms of hydrate-bearing sediments during gas production.

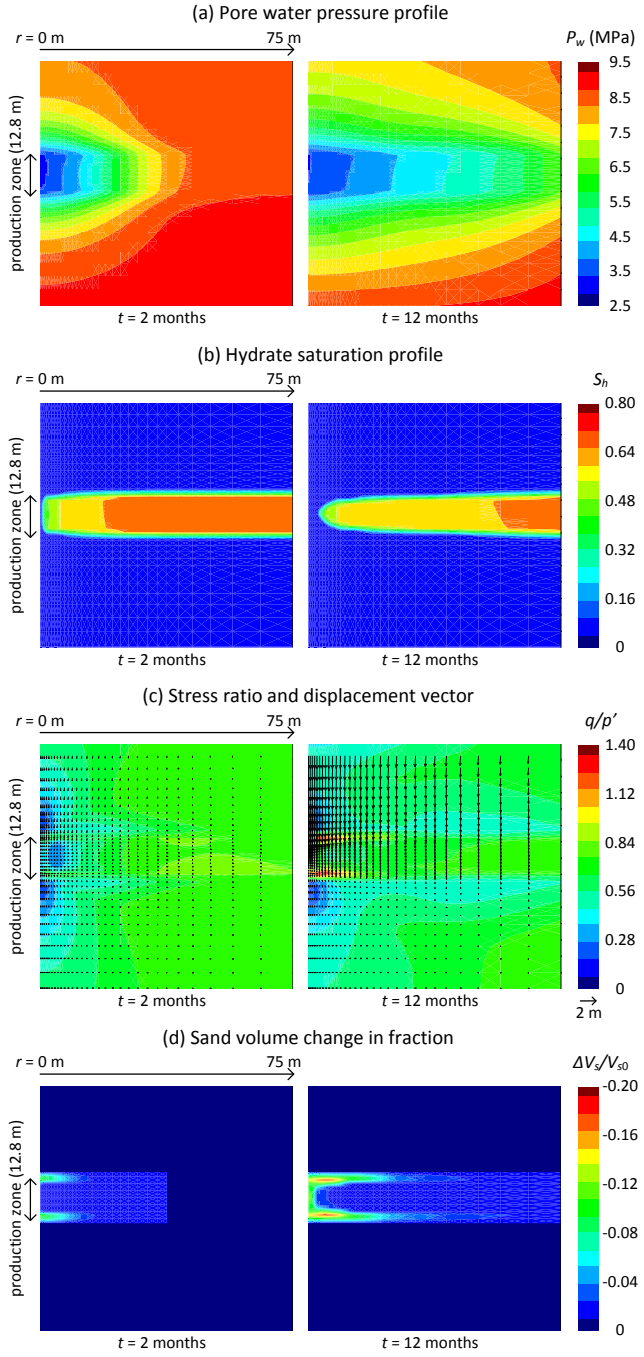

Figure 3. Spatial and temporal changes in (a) pore water pressure, (b) hydrate saturation, (c) stress ratio and (d) sand volume.

Fig. 4a shows the produced sand volume, that is, volume of sand flow collected at the well, with variability associated with the variability in the permeability and stress-strain curves. There are two key findings. Firstly, sand production does not appear to cease. This is because constantly evolving hydrate dissociation keeps hydraulic gradient and shear deformation continuously grow, leading to ever-increasing sand mobilization. Therefore, when sand screen is installed and blocks the sand flow at the well, there can be continuous stress change around the well and also prolonged accumulation of flowing sands at the well. Secondly, the variability in the permeability and stress-strain curves leads to appreciable range in the prediction. In order to better understand how each properties affect sand production, the analyses are used to determine the first-order sensitivity indecies (Sobol', 1993), implying how much contribution each property has to the overall sand production. Fig. 4b shows the evaluated first-order sensitivity and its change over time. It is found that the permeability dominantly affects sand production. It has to be mentioned, however, in the early stage the effective permeability is more important than the intrinsic permeability but with time the intrinsic permeability becomes more important. This reflects the dynamic change of hydrate reservoir behavior and also suggests that it is essential to rigorously examine how permeability changes with hydrate dissociation.

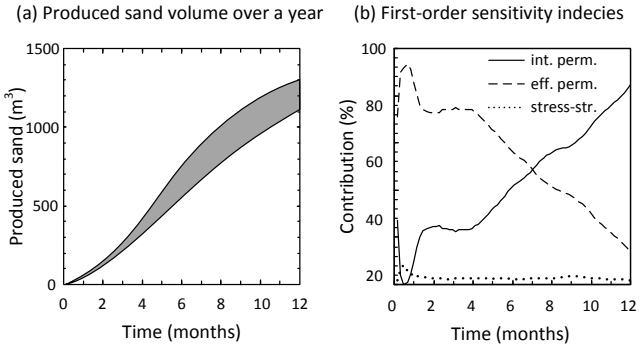

Figure 4. (a) volume of produced sand and (b) contribution from varied properties.

4. CONCLUDING REMARKS

This study investigated how sand migration could occur during one-year gas production from gas hydrate reservoir in the Prudhoe Bay Unit on the Alaska North Slope. There are mainly three key findings:

- a large amount of sand flow comes from the vicinity of the interface between hydrate-bearing sand and silty-clay layers because of large shear deformation caused by difference in permeability and stress-strain curves;

- sand mobilization in these area appears to continuously grow because of evolving hydrate dissociation front; and
- sand production is dominantly affected by the sediments' permeability and its change due to hydrate dissociation needs to be carefully evaluated.

Due to inherent uncertainties in the in-situ properties, model parameters and assumptions required for numerical modeling, quantitative prediction of sand production is always a challenge. This study showed qualitatively how sand production may occur. These three findings corroborate that further studies are necessary to offer more accurate prediction of sand production and thus to conduct successful one-year long gas production in the Prudhoe Bay Unit.

5. ACKNOWLEDGEMENT

This study is conducted as a part of JOGMEC and NETL collaboration funded by the Ministry of Economy, Trade and Industry of Japan and the U.S. Department of Energy through a support contract with Leidos Research Support Team (LRST). Neither the United States Government nor any agency thereof, nor any of their employees, nor LRST, nor any of their employees, makes any warranty, expressed or implied, or assumes any legal liability or responsibility for the accuracy, completeness, or usefulness of any information, apparatus, product, or process disclosed, or represents that its use would not infringe privately owned rights. Reference herein to any specific commercial product, process, or service by trade name, trademark, manufacturer, or otherwise, does not necessarily constitute or imply its endorsement, recommendation, or favoring by the United States Government or any agency thereof. The views and opinions of authors expressed herein do not necessarily state or reflect those of the United States Government or any agency thereof.

6. REFERENCES

Boswell, R., Collett, T.S., 2011. Current perspectives on gas hydrate resources. *Energy & Environmental Science* 4, 1206–1215.

Chen, L., Feng, Y., Okajima, J., Komiya, A., Maruyama, S., 2018. Production behavior and numerical analysis for 2017 methane hydrate extraction test of shenhu, south china sea. *Journal of Natural Gas Science and Engineering* 53, 55 – 66.

Dallimore, S.R., Wright, J.F., Yamamoto, K., Bellefleur, G., 2012. Proof of concept for gas hydrate production using the depressurization technique, as established by the JOGMEC/NRCan/Aurora Mallik 2007-2008 gas hydrate production research well program. *Bulletin of the Geological Survey of Canada* 601, 1–15. doi:10.4095/292079.

Konno, Y., Fujii, T., Sato, A., Akamine, K., Naiki, M., Masuda, Y.,Yamamoto, K., Nagao, J., 2017. Key findings of the world's first offshore methane hydrate production test off the coast of Japan: Toward future commercial production. *Energy & Fuels* 31, 2607–2616.

Kubo, Y., Mizuguchi, Y., Inagaki, F., Yamamoto, K., 2014. A new hybrid pressure-coring system for the drilling vessel chikyu. *Scientific Drilling* 17, 37–43. doi:10.5194/sd-17-37-2014.

Masuda, Y., Naganawa, S., Fujita, K., Sato, K., Hayashi, Y., 1999. Modeling and experimental studies on dissociation of methane gas hydrates in berea sandstone cores, in: Proceedings of the 3rd International Conference on Gas Hydrate, pp. 23–31.

Moridis, G.J., Collett, T.S., Boswell, R., Kurihara, M., Reagan, M.T., Koh, C., Sloan, E.D., 2009. Toward production from gas hydrates: Current status, assessment of resources, and simulation-based evaluation of technology and potential. *SPE Reservoir Evaluation & Engineering* 12, 745–771. doi:10.2118/114163-pa.

Myshakin, E.M., Seol, Y., Lin, J.S., Uchida, S., Collett, T.S., Boswell, R., 2019. Numerical simulations of depressurization-induced gas production from an interbedded turbidite gas hydrate-bearing sedimentary section in the offshore India: Site NGHP-02-16 (Area-b). *Marine and Petroleum Geology* 108, 619 – 638.

Priest, J.A., Hayley, J.L., Smith, W.E., Schultheiss, P., Roberts, J.,2019. PCATS triaxial testing: Geomechanical properties of sediments from pressure cores recovered from the bay of Bengal during expedition NGHP-02. *Marine and Petroleum Geology* 108, 424– 438. doi:10.1016/j.marpetgeo.2018.07.005.

Santamarina, J., Dai, S., Terzariol, M., Jang, J., Waite, W., Winters, W., Nagao, J., Yoneda, J., Konno, Y., Fujii, T., Suzuki, K., 2015. Hydro-bio-geomechanical properties of hydrate-bearing sediments from Nankai trough. *Marine and Petroleum Geology* 66, 434-450. doi:10.1016/j.marpetgeo.2015.02.033.

Sobol', I.M., 1993. Sensitivity estimates for nonlinear mathematical models. *Mathematical Modeling and Computational Experiment* 1, 407–414.

Uchida, S., Klar, A., Yamamoto, K., 2016a. Sand production model in gas hydrate-bearing sediments. *International Journal of Rock Mechanics and Mining Sciences* 86, 303–316.

Uchida, S., Lin, J.S., Myshakin, E.M., Seol, Y., Boswell, R., 2019a. Numerical simulations of sand migration during gas production in hydrate-bearing sands interbedded with thin mud layers at site NGHP-02-16. *Marine and Petroleum Geology* 108, 639 – 647.

Uchida, S., Seol, Y., Yamamoto, K., 2019b. Variance-based determination of dominant model parameters for sand migration in homogeneous gas hydrate-bearing reservoir. Japanese Geotechnical Society Special Publication 7, 360–365.

Uchida, S., Soga, K., Yamamoto, K., 2012. Critical state soil constitutive model for methane hydrate soil. *Journal of Geophysical Research* 117, 1–13.

Uchida, S., Xie, X.G., Leung, Y.F., 2016b. Role of critical state framework in understanding geomechanical behavior of methane hydrate-bearing sediments. *Journal of Geophysical Research: Solid Earth* 121, 5580–5595.

Yamamoto, K., Wang, X.X., Tamaki, M., Suzuki, K., 2019. The second offshore production of methane hydrate in the Nankai Trough and gas production behavior from a heterogeneous methane hydrate reservoir. *RSC Advances* 9, 25987–26013.

Yoneda, J., Masui, A., Konno, Y., Jin, Y., Kida, M., Katagiri, J., Nagao, J., Tenma, N., 2017. Pressure-core-based reservoir characterization for geomechanics: Insights from gas hydrate drilling during 2012–2013 at the eastern Nankai Trough. *Marine and Petroleum Geology* 86, 1–16.

Yoneda, J., Oshima, M., Kida, M., Kato, A., Konno, Y., Jin, Y., Tenma, N., 2019. Consolidation and hardening behavior of hydrate-bearing pressure-core sediments recovered from the Krishna–Godavari Basin, offshore India. *Marine and Petroleum Geology* 108, 512 – 523.